science, engineering and health studies

Research Article

Science, Engineering and Health Studies
https://lio1.tci-thaijo.org/index.php/sehs
ISSN (Online): 2630-0087

Development of a low-cost continuous passive motion machine for the enhanced rehabilitation of elderly individuals with osteoarthritis

Siwasit Pitjamit[1,2], Parida Jewpanya[1,2], Pakpoom Jaichomphu[1,2], Pinit Nuangpirom[3], Kattareeya Prompreing[4], Chakrit Wiboonsuntharangkoon[5,6], and Norrapon Vichiansan[7]*

[1] Center of Excellence, Faculty of Engineering, Rajamangala University of Technology Lanna, Tak 63000, Thailand
[2] Department of Industrial Engineering, Faculty of Engineering, Chiang Mai University, Chiang Mai 50200, Thailand
[3] Department of Electrical Engineering, Faculty of Engineering, Rajamangala University of Technology Lanna, Tak 63000, Thailand
[4] Faculty of Business Administrations and Liberal Arts, Rajamangala University of Technology Lanna, Chiang Mai 50300, Thailand
[5] Biomedical Engineering and Innovation Research Center, Chiang Mai University, Chiang Mai 50200, Thailand
[6] Biomedical Engineering Institute (BMEI), Chiang Mai University, Chiang Mai 50200, Thailand
[7] Multidisciplinary Center, Faculty of Engineering, Chiang Mai University, Chiang Mai 50200, Thailand

***Corresponding author**:
Parida Jewpanya
parida.jewpanya@cmu.ac.th

***Received**: 17 May 2024*
***Revised**: 21 July 2024*
***Accepted**: 28 August 2024*
***Published**: 14 November 2025*

***Citation**:
Pitjamit, S., Jewpanya, P., Jaichomphu, P., Nuangpirom, P., Prompreing, K., Wiboonsuntharangkoon, C., & Vichiansan, N. (2025). Development of a low-cost continuous passive motion machine for the enhanced rehabilitation of elderly individuals with osteoarthritis. Science, Engineering and Health Studies, 19, 25040007.

ABSTRACT

With the increasing global prevalence of osteoarthritis and the expansion of the aging population, this research presents an innovative low-cost continuous passive motion (CPM) machine tailored to meet the specific rehabilitation needs of elderly individuals, particularly those grappling with osteoarthritis. The primary aim of this study was to address the increasing demand for effective knee rehabilitation tools in this population. The newly developed CPM machine offers a versatile range of features, allowing users to customize the treatment times, knee joint motion angles, and speed levels. Statistical analysis demonstrated the accuracy and reliability of the machine, which is designed for knee rehabilitation in elderly individuals. A one-way ANOVA showed no significant difference between the machine's performance and control units, both in terms of the angle replication and time measurements. The precision and consistency of the device were underscored by the close alignment of the CPM machine with goniometer measurements and the minimal error in time measurements, which did not exceed 2.66% and 0.13% during the first 20 minutes of use. These statistical findings confirm the efficacy of the CPM machine in delivering reliable and accurate knee rehabilitation, with potential benefits for improving quality of life and mobility.

Keywords: osteoarthritis; knee rehabilitation; continuous passive motion (CPM); elderly patients; healthcare technology

1. INTRODUCTION

Osteoarthritis (OA) is a prevalent and debilitating degenerative joint disorder, and it particularly affects the aging population. Its impact is widespread, causing substantial pain, impaired mobility, and a diminished quality of life for those affected (Hunter et al., 2014). As the most common form of arthritis, osteoarthritis represents a significant public health challenge (Neogi, 2013). The knee joint often bears the brunt of OA, leading to considerable morbidity and imposing substantial economic burdens on healthcare systems worldwide. In the quest to alleviate the effects of this condition, continuous passive motion (CPM) therapy has emerged as a valuable rehabilitation modality, aiding in the restoration of knee joint mobility in individuals with osteoarthritis. However, effective, conventional CPM devices are often prohibitively expensive, limiting their accessibility for elderly individuals or those with financial constraints.

Designing a low-cost CPM machine for knee rehabilitation is crucial for addressing the challenges faced by the elderly, especially those with osteoarthritis. This design should prioritize affordability and precision in replicating knee joint motion. The versatile features of the machine, including customizable treatment times, motion angles, and speed levels, make it a promising solution (Cross et al., 2014; Lee et al., 2022). This approach aligns with the growing demand for accessible and efficient healthcare technologies, particularly in the context of an aging population (Brosseau et al., 2017). This study aims to tackle this issue by developing an economical CPM machine that is specifically tailored to the rehabilitation needs of elderly individuals battling osteoarthritis. The primary objective of this machine is to facilitate rehabilitation by providing a controlled and customizable range of motion suitable for osteoarthritis patients (Kim et al., 2023). By ensuring affordability and user-friendliness, this device is intended to enhance access to rehabilitative interventions, ultimately promoting improved knee joint mobility and reduced pain among the elderly population affected by osteoarthritis.

In this article, a comprehensive exploration of the design, development, and functionality of the low-cost CPM machine is presented. The device features adjustable speeds and a range of motions that allow rehabilitation sessions to be tailored to the unique needs of individuals with osteoarthritis, with a specific focus on optimizing user experience and adherence to prescribed rehabilitation protocols (Cherian et al., 2015). Central to its design is the integration of a touch-screen-based controller, providing a user-friendly interface for seamless interactions and the customization of rehabilitation sessions (Berry et al., 2002; Almusawi & Husi, 2021). By achieving cost-effectiveness without compromising functionality, this low-cost CPM machine shows promise in enhancing knee joint mobility and the overall quality of life for elderly individuals suffering from osteoarthritis.

2. MATERIALS AND METHODS

2.1 Block diagram for a continuous passive motion (CPM) machine

The block diagram in Figure 1 outlines the core functioning of the CPM machine. User input is received via a 4.3-inch Arduino SPI I2C TFT Touchscreen 800x480 LCD Display, which is transmitted to the central microcontroller board (ER-TFTMC043-7). This microcontroller acts as the control hub, processing touch-screen commands and coordinating subsequent actions. It interacts with the power converter, which controls the DC motor's rotation, while gear boxes regulate the motor revolutions according to preset parameters. This gearing system enhances motor torque, ensuring controlled knee joint movements in line with the chosen speed setting (Almusawi & Husi, 2021). For safety, limit switches restrict movement within the defined range. An encoder continuously monitors and confirms the mechanism's adherence to parameters until the user's set treatment duration is met.

2.2 CPM Machine flowchart

The process starts with a zero-degree calibration, the "Original Point," which is typically achieved in manual mode. Then, treatment parameters (speed, time, and degree) are configured in the settings mode, spanning a 0–123-degree range, with treatment durations from 0–24 and speed levels from 1 to 100 (corresponding to approximately 0.1 to 10 meters per minute). Transitioning to auto run, the treatment data are displayed for accuracy, and activating "Start" initiates the CPM machine. The screen updates the treatment status until the preset duration is met, after which the CPM operation stops (Saputra & Iskandar, 2011).

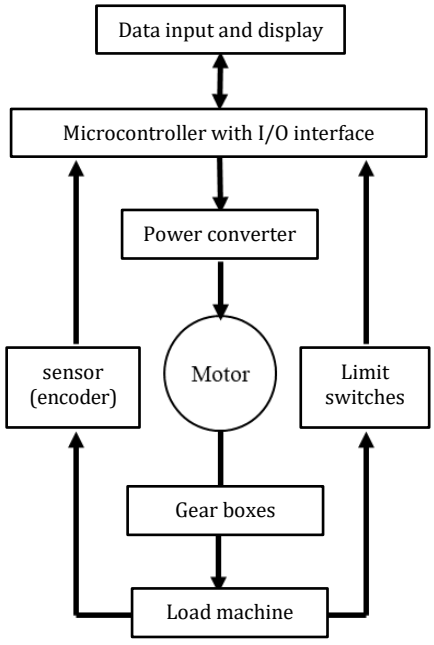

Figure 1. Block diagram of the CPM machine

2.3 Design of CPM machine

The CPM machine design consists of five key components: Part 1 for data input and display, Part 2 for data feedback, Part 3 as the motor driver, Part 4 for motor and gear reduction, and Part 5, the mechanical device components. These components collectively manage the data input, the feedback, the motor control, and the mechanical structure responsible for knee joint motion during the rehabilitation process.

In the process of designing this CPM machine, the initiation begins with the development of the mechanical components, followed by the integration of the motor, motor drive unit, data feedback system, and data input and display subsystems.

2.4 Load machine

The mechanical design of the CPM machine uses the slider–crank principle, which is chosen for its ability to closely imitate the knee joint's natural movements, including extension and flexion. This mechanism allows for coordinated positional and rotational adjustments, replicating the essential actions of the knee joint, as shown in Figure 2a. The design and construction of the CPM machine rely on the slider–crank mechanism, as seen in Figure 2a. Umchid and Taraphongphan (2016), and Wu et al. (2021) provide crucial information about the average lengths of the femur (OA) and tibia (AB), as shown in Figure 2b, which is essential for determining the dimensions of the ball screw (OB). The ball screw is vital for converting rotational motion into linear movement. The resulting CPM machine offers a comprehensive range of standard settings, accommodating patients with heights ranging from 130 cm to 190 cm. The adjustability for femur and tibia lengths spans from approximately 32 cm to 47 cm, ensuring adaptability to various patient heights.

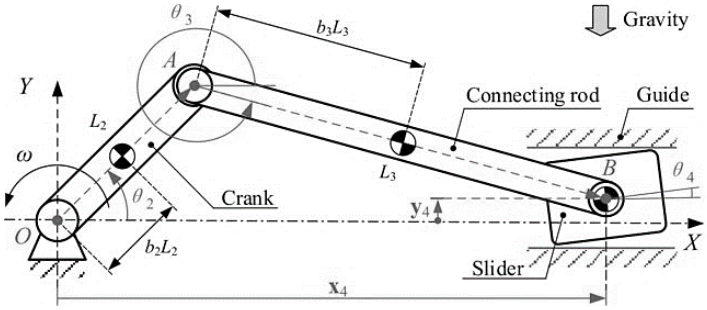

(a)

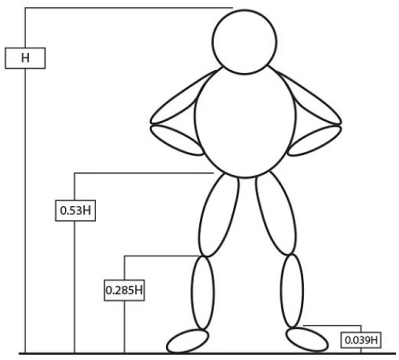

(b)

Figure 2. Slider–crank mechanism and anthropometric relationships
Note: (a) setup of the slider–crank mechanism featuring a translational clearance joint; (b) relationship between femur length, tibia length, and patient height

In Figure 2a, the crank angle θ is located at the point of rotation of the crank and is measured in degree (°). The linear speed ν of the slider is measured in meters per minute (m/min). The angular velocity ω is measured in radians per second (rad/s), and the acceleration is given in meters per second squared (m/s^2). The slider site is where the linear motion occurs, translating the rotational motion into linear movement.

The mechanism synthesis and analysis of the slider–crank system involves fundamental equations that govern its behavior, including its position, velocity, and acceleration (Sun et al., 2023). The position of the slider (p) in relation to the crank angle (θ) and connecting rod length (L) can be determined using Equation 1:

$$p = L \cdot (1 - \cos(\theta)) \quad (1)$$

Additionally, the linear velocity (v) of the slider can be expressed as Equation 2:

$$v = -L \cdot \omega \cdot \sin(\theta) \quad (2)$$

where ω represents the angular velocity of the crank. For acceleration analysis, Equation 3 is applied, with α denoting the angular acceleration of the crank:

$$a = -L \cdot \alpha \cdot \cos(\theta) - L \cdot \omega^2 \cdot \sin(\theta) \quad (3)$$

These equations allow for a comprehensive understanding of the slider–crank mechanism's performance, helping to ensure its suitability for knee rehabilitation applications.

Additionally, calculations for torque and force, which are required for the linear actuator, are conducted. Once the optimal dimensions for the femur section, tibia section, and ball screw are determined, the 3D mechanical structure of the CPM machine is created using SolidWorks software, as shown in Figure 3a.

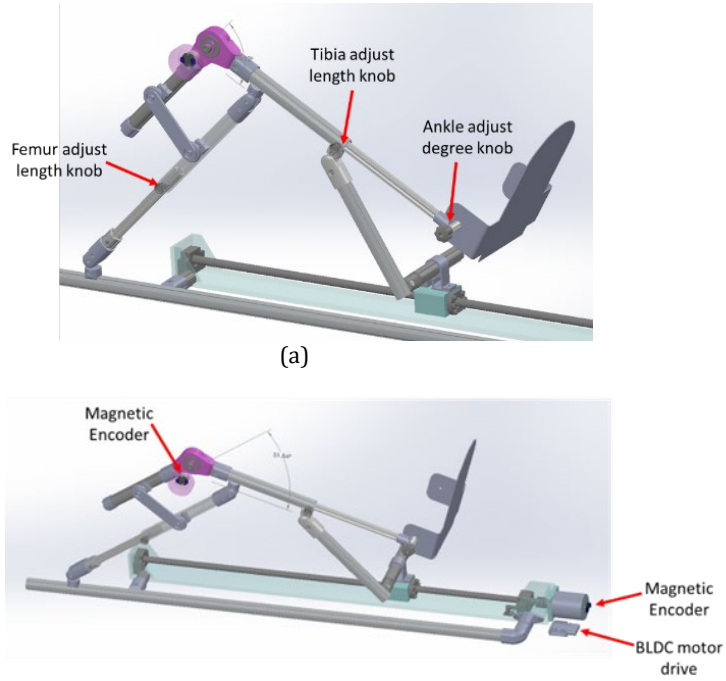

Figure 3. Design of the CPM Machine and the DC motor installation position in the CPM machine

2.5 DC motor

The chosen motor possessed the following specific attributes: a speed of 110 rpm, a voltage rating of 24 V, and an electrical power rating of 45 W. The speed of 110 rpm was selected to ensure an optimal balance between rotational speed and torque for the CPM machine's requirements. This speed allows the machine to provide the smooth and controlled motion that is necessary for effective knee rehabilitation. Subsequently, the motor's speed and torque characteristics were determined after it interacted with a gear set. The gear set reduces the motor's rotational speed while increasing its torque output. These characteristics are fundamental to the motor's performance and efficiency (Parra et al., 2022). They are closely related via the mechanical power, as shown in Equation 4:

$$P = T \cdot \omega / 1000 \quad (4)$$

where P is the mechanical power (Watt, W), T is the torque (Newton meter, Nm), and ω is the angular velocity or rotational speed (radian per second, rad/s).

The required power of the motor was calculated based on the estimated torque and speed requirements of the CPM machine. Although the exact force, torque, and angular velocity were initially unknown, they were approximated using the expected load that the CPM machine would handle during typical operation. The angular velocity (ω) was derived from the motor speed (110 rpm), which converts to approximately 11.52 rad/s (using the conversion factor $\frac{2\pi\ radians}{60\ seconds}$). The torque ($T$) was then estimated based on the mechanical design considerations and the anticipated resistance during knee movements.

This selected motor will be placed on the CPM machine's foundational base, as depicted in Figure 3b; it plays a foundational role in the design of the motor's drive unit. The motor's specifications ensure that it can provide the necessary power and control for effective knee joint rehabilitation in elderly patients.

2.6 Power drive motor

A planetary reduction brushless DC motor, 24V, 45W, 61mm driver board, identified as model B10-42BL24578B, was selected to control the motor operations. This control board is equipped with the capacity to provide voltage to a motor within the range of 12 to 24 VDC (Rahman et al., 2018). It can deliver a maximum current of 40 amps and offers speed control through a pulse width modulation (PWM) signal.

2.7 Rotary encoder

To verify and precisely measure the operational angle of the machine, a rotary encoder sensor, Model AS5600, was chosen. This rotary encoder sensor was selected to ensure the acquisition of accurate values across every degree of motion. The sensor's output is configured to provide pulse signals, where each pulse corresponds to a single degree of movement. In other words, a 1-pulse output is synonymous with a 1-degree increment, ensuring the precision of the angle measurement. The relationship between the number of pulses (N_{pulses}) and the angular movement (θ) can be described, as shown in Equation 5:

$$N_{pulses=}\ \theta \quad (5)$$

where N_{pulses} represents the number of pulses generated by the encoder, and θ is the angular movement in degrees. This configuration allows for precise angle measurements. The encoder's installation location on the CPM machine is shown in Figure 3b.

2.8 Data input and display design

The design features a touch screen interface for input and data protection, including settings for knee joint movement (0–123 degrees), the treatment duration (0–24), and speed

levels (0–100), which are displayed on an integrated LCD screen. The operation of the CPM machine is categorized into three modes: 1) a manual mode for configuring the default angle (0 degrees) with the flexibility for personalized adjustments (Figure 4a), 2) a setting mode for specifying treatment parameters (duration, knee range, and speed) (Figure 4b), and 3) an auto-run mode for confirming the treatment data obtained from the setting mode (Figure 4c). The CPM machine's operations are initiated upon pressing "Start" and treatment progress is tracked.

(a) (b) (c)

Figure 4. Touch screen interface in different modes; (a) Manual mode, (b) setting mode, and (c) auto-run mode

3. RESULTS

The low-cost CPM machine allows for continuous and gradual knee joint movement within a 0–123 degree range, with speed adjustability from 30–150 degrees per second across 0–100 speed levels. It offers customizable treatment durations that are suitable for various therapeutic protocols, accommodating sessions typically ranging from several minutes to up to 24. Leg length adjustments cater to users with heights of 130–190 cm, and the inclusion of a touch screen and remote control enhances user-friendliness, simplifying the experience. For a visual representation (see Figure 5).

3.1 Motion degree testing

A comprehensive assessment was conducted to validate the low-cost CPM machine's motion capabilities by comparing its range of motion angles with goniometer measurements (Umchid & Taraphongphan, 2016; Bible et al., 2009). The results, presented in Table 1, demonstrate that the margin of error for angular measurements, particularly within the 0–123 degree range, consistently fell below 2.66%. This finding highlights the machine's remarkable precision, underscoring its reliability for clinical use.

Figure 5. The final low-cost cpm machine

Table 1. Comparative analysis of angular measurements obtained from the encoder and goniometer devices

Replication status	Angle measured from goniometer (degree)	Average angle (degree)	Percentage error (%)
No. 1	0		
No. 2	0		
No. 3	0	0.00	0.00
No. 4	0		
No. 5	0		
No. 1	14		
No. 2	15		
No. 3	15	14.60	2.66
No. 4	14		
No. 5	15		
No. 1	30		
No. 2	30		
No. 3	30	29.83	0.56
No. 4	29		
No. 5	30		
No. 1	45		
No. 2	46		
No. 3	44	45.00	0.00
No. 4	45		
No. 5	45		
No. 1	59		
No. 2	59		
No. 3	61	59.80	0.33
No. 4	60		
No. 5	60		
No. 1	75		
No. 2	76		
No. 3	76	75.20	0.26
No. 4	75		
No. 5	74		
No. 1	91		
No. 2	90		
No. 3	89	89.80	0.22
No. 4	90		
No. 5	89		
No. 1	104		
No. 2	104		
No. 3	105	104.80	0.19
No. 4	105		
No. 5	106		
No. 1	119		
No. 2	120		
No. 3	121	120.40	0.33
No. 4	120		
No. 5	122		
No. 1	123		
No. 2	124		
No. 3	122	123.00	0.00
No. 4	124		
No. 5	122		

Each "No." (e.g., No. 1 to No. 5) represents a separate measurement session or trial conducted to gather data on the angular measurements from both the encoder and goniometer devices.

The analysis of the machine's angle measurement data involved a comparative examination of differences between the control unit and the machine. This was carried out using a one-way ANOVA to assess variance and investigate variations in the angles of the controlled variables. The primary hypothesis (H_0) was formulated as H_0: $\mu_1 = \mu_2$, with the secondary hypothesis (H_α) as H_α: $\mu_1 \neq \mu_2$. The results of the experiment, presented in Table 2, revealed a p-value exceeding 0.05, equaling 0.998. This signifies that, at a 95% confidence level, there exists no statistically significant difference in the time measured during the actual test. Further support for this conclusion is derived from grouping the data, where both control and test groups are labeled as "A," indicating that the testing times are not significantly different. This observation is reinforced with reference to Figure 6a, which displays the Tukey simultaneous 95% confidence interval (CI) value. It demonstrates that the angles in both the control and test groups are not distinct, as the CI overlaps with the zero line.

The evaluation of data quality was conducted using a residual plot graph, as depicted in Figure 6b. The examination of the normal probability plot within the graph confirmed the normal distribution of the data. Furthermore, the versus fits graph was instrumental in assessing the constant variance in the error values, demonstrating a consistent pattern across all groups. Additionally, the versus order graph, which examines data independence, displayed well-controlled, normally distributed data. These observations collectively underscore the reliability and robustness of the dataset.

Table 2. Comparative analysis of angle differences between the control variables and the CPM machine

Source	Df	Adj ss	Adj ms	F-value	P-value
Factor	1	0.0	0.02	0.00	0.998
Error	18	34222.1	1901.23		
Total	19	34222.1			
Means					
Factor	N	Mean	SD	95% CI	
Desired	10	66.3	43.6	(37.3, 95.3)	
Actual	10	66.2	43.7	(37.3, 95.2)	
Grouping information using the Tukey method and the 95% CI					
Factor	N	Mean	Grouping		
Desired	10	66.3	A		
Actual	10	66.2	A		

Note: *pooled SD = 43.6030; means that do not share a letter are significantly different

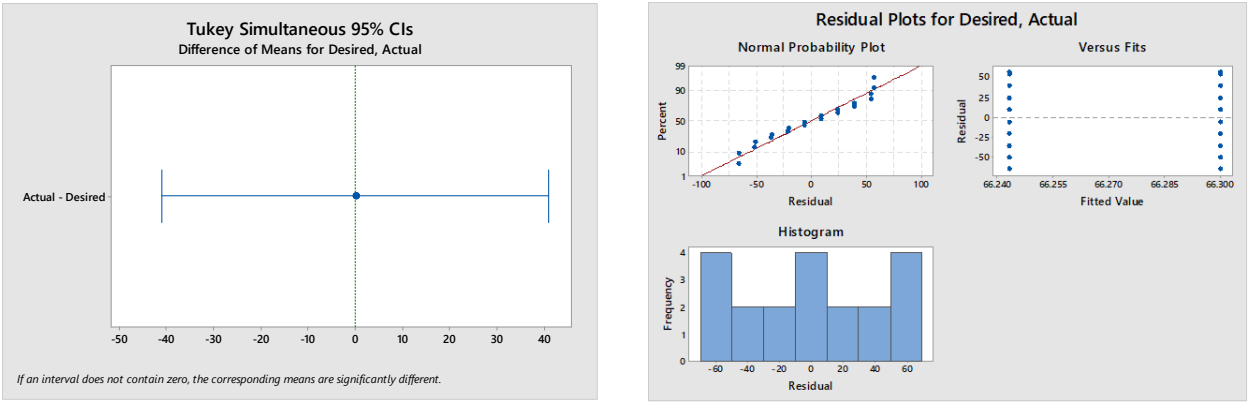

(a) (b)

Figure 6. Variance test results for angle differences; (a) Tukey simultaneous analysis and, (b) residual plots of variance tests to compare the angle differences between the control variables and the machine

3.2 Time testing

The CPM machine's functionality includes flexible treatment duration settings ranging from 0 to 24. To assess its performance, a thorough examination compared the CPM machine's preset treatment durations with actual stopwatch measurements. The detailed results, presented in Table 2, underscore the machine's temporal accuracy and reliability in adhering to predefined treatment durations, offering valuable insights into its temporal precision. An analysis of the data in Table 3 reveals consistently minimal variations between the time intervals recorded by the CPM machine and those from the stopwatch, particularly within the initial 20 min. These observations highlight the CPM machine's precise temporal performance and its reliability in maintaining prescribed treatment durations.

Table 3. Comparison of time measurements between the CPM machine and a stopwatch

Replication status	Time measured by a stopwatch (min)	Average angle (degree)	Percentage error (%)
No. 1	5.01		
No. 2	5.00		
No. 3	5.00	5.00	0.13
No. 4	5.02		
No. 5	4.99		
No. 1	10.01		
No. 2	10.00		
No. 3	9.98	9.99	0.05
No. 4	10.00		
No. 5	10.00		
No. 1	20.00		
No. 2	20.00		
No. 3	20.01	20.00	0.02
No. 4	20.01		
No. 5	20.00		
No. 1	30.00		
No. 2	30.01		
No. 3	30.01	30.00	0.02
No. 4	30.01		
No. 5	30.00		

The time measurements were analyzed to compare data variations between the CPM machine and the control unit using one-way ANOVA. The primary hypothesis (H_0: $\mu_1 = \mu_2$) and secondary hypothesis (H_α: $\mu_1 \neq \mu_2$) were formulated. The results in Table 4 show a p-value greater than 0.05 (equal to 1), indicating no statistically significant difference in the time measurements at a 95% confidence level. This conclusion was further supported by the grouping analysis, where both the control and experimental groups were labeled as "A," signifying no significant time differences. This observation was consistent with Figure 7a, illustrating the simultaneous Tukey 95 values, where the confidence intervals (CI) intersected the zero line.

The residual plot graph, shown in Figure 7b, confirms the normal distribution of data through the normal probability plot. The versus fits graph reveals consistent variance in error values across all groups, while the versus order graph demonstrates well-controlled and normally distributed data, affirming the dataset's reliability and quality.

Table 4. Comparative analysis of temporal differences between the control variables and the CPM machine

Source	Df	Adj ss	Adj ms	F-value	P-value
Factor	1	0.000	0.000	0.00	1.000
Error	6	737.720	122.953		
Total	7	737.720			
Means					
Factor	N	Mean	SD	95% CI	
Control	4	16.25	11.09	(2.68, 29.82)	
Time	4	16.25	11.09	(2.69, 29.82)	
Grouping information using the Turkey method and 95% CI					
Factor	N	Mean	Grouping		
Control	4	16.25	A		
Time	4	16.25	A		

Note: pooled SD = 11.0884; means that do not share a letter are significantly different

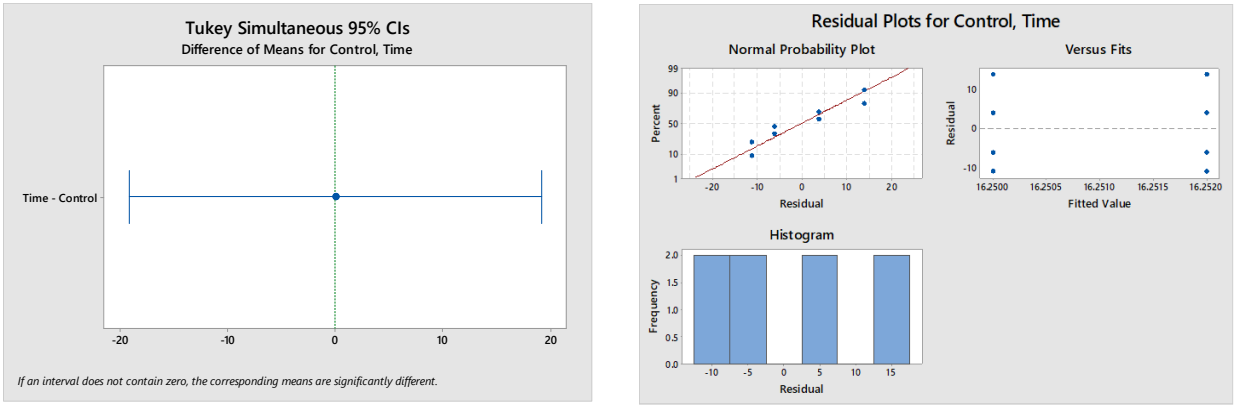

(a) (b)

Figure 7. Analysis of variance for temporal differences between control variables and the CPM Machine; (a) simultaneous tukey and, (b) residual plots

4. DISCUSSION

Regarding angular precision and machine reliability, the in-depth analysis of the low-cost CPM machine's angular precision underscores its remarkable reliability in delivering precise motion control, as evidenced by the consistent error margin of less than 2.66%. This precision aligns with the fundamental objective of osteoarthritis management (Hunter et al., 2014). It is essential to ensure that the machine effectively addresses the individual and socioeconomic impact of osteoarthritis (Cross et al., 2014). Given the economic burden of this condition, the machine's reliability in providing accurate angular measurements is of significant value, promising improved outcomes for patients (Berry et al., 2002).

The temporal accuracy and treatment duration—an equally critical aspect of the CPM machine's performance—were also evaluated. Our findings reveal that the machine consistently recorded time intervals with discrepancies well below 0.13% during the initial 0–30 min of treatment. This level of temporal precision is pivotal in adhering to the recommended osteoarthritis management guidelines and is consistent with the clinical relevance of precise timing in treatments. The machine's ability to effectively adhere to predefined treatment durations therefore holds substantial promise in the context of osteoarthritis rehabilitation (Johnston et al., 1990; Szabo et al., 2023).

The machine's user-friendliness is an important facet of its performance, and the analysis suggests that the efficient touch screen interface makes it highly accessible for elderly patients suffering from osteoarthritis. This aspect of the CPM machine aligns with the user-centric approach recommended by experts in osteoarthritis management (Cherian et al., 2015). Furthermore, its adaptability is showcased by its ability to accommodate variations in patient height and limb length. The adjustable femur and tibia lengths, ranging from 32 cm to 47 cm, cater to a broad range of elderly individuals, ensuring that it aligns with their specific anatomical needs (Herbold et al., 2014). Such adaptability is essential for addressing the diverse requirements of osteoarthritis patients. The low-cost CPM machine has significant potential to revolutionize osteoarthritis management for the elderly. These machines offer multifaceted opportunities that can transform the way we approach the treatment of this debilitating condition.

As suggested by prior research (Mille et al., 2023; Brosseau et al., 2017), CPM machines provide multifaceted benefits for elderly osteoarthritis patients. They offer non-invasive pain relief and enhance joint functionality. In the context of postoperative care, CPM machines accelerate recovery, minimizing complications. Their adaptability and automated exercises ensure personalized, consistent, and long-term management. These advantages collectively enhance the quality of life for elderly osteoarthritis patients, representing a notable healthcare advancement.

5. CONCLUSION

In conclusion, the low-cost CPM machine tailored for elderly individuals, particularly those with osteoarthritis, demonstrates substantial promise. It offers user-friendly features, including customizable treatment parameters. Rigorous testing showcased its impressive accuracy in replicating knee joint angles and maintaining precise time measurements. Statistical analysis, conducted via one-way ANOVA, revealed no significant differences between the CPM machine and control units in terms of both the angle replication and the time measurements. The close alignment with goniometer measurements and minimal time measurement errors, which did not exceed 2.66% and 0.13% within the initial 20 minutes of use, underscore the machine's precision. This CPM machine has the potential to significantly enhance knee rehabilitation for the elderly, improving their mobility and overall wellbeing. As the global prevalence of osteoarthritis and aging populations continue to rise, this low-cost CPM machine offers a valuable contribution to effective knee joint recovery, presenting opportunities for advancements in rehabilitative technology to address diverse patient needs.

ACKNOWLEDGMENTS

The authors are grateful to the Fundamental Fund for their financial support in fiscal year 2023, under the basic research fund type, project code 2566FFP153. This funding

facilitated the research project titled "The Construction of Knee Motion Testing Device for Elderly." The authors also extend their sincere appreciation to the dedicated research team whose expertise and commitment were instrumental in the successful development of the knee motion testing device.

REFERENCES

Almusawi, H., & Husi, G. (2021). Design and development of continuous passive motion (CPM) for fingers and wrist grounded-exoskeleton rehabilitation system. *Applied Sciences*, *11*(2), Article 815. https://doi.org/10.3390/app11020815

Berry, D. J., Harmsen, W. S., Cabanela, M. E., & Morrey, B. F. (2002). Twenty-five-year survivorship of two thousand consecutive primary charnley total hip replacements: Factors affecting survivorship of acetabular and femoral components. *The Journal of Bone & Joint Surgery*, *84*(2), 171–177. https://doi.org/10.2106/00004623-200202000-00002

Bible, J. E., Simpson, A. K., Biswas, D., Pelker, R. R., & Grauer, J. N. (2009). Actual knee motion during continuous passive motion protocols is less than expected. *Clinical Orthopaedics and Related Research*, *467*(10), 2656–2661. https://doi.org/10.1007/s11999-009-0766-1

Brosseau, L., Taki, J., Desjardins, B., Thevenot, O., Fransen, M., Wells, G. A., Mizusaki Imoto, A., Toupin-April, K., Westby, M., Álvarez Gallardo, I. C., Gifford, W., Laferrière, L., Rahman, P., Loew, L., De Angelis, G., Cavallo, S., Mehdi Shallwani, S., Aburub, A., Bennell, K. L., … & McLean, L. (2017). The Ottawa panel clinical practice guidelines for the management of knee osteoarthritis. Part two: Strengthening exercise programs. *Clinical Rehabilitation*, *31*(5), 596–611. https://doi.org/10.1177/0269215517691084

Cherian, J. J., Jauregui, J. J., Banerjee, S., Pierce, T., & Mont, M. A. (2015). What host factors affect aseptic loosening after THA and TKA? *Clinical Orthopaedics and Related Research*, *473*(8), 2700–2709. https://doi.org/10.1007/s11999-015-4220-2

Cross, M., Smith, E., Hoy, D., Nolte, S., Ackerman, I., Fransen, M., Bridgett, L., Williams, S., Guillemin, F., Hill, C. L., Laslett, L. L., Jones, G., Cicuttini, F., Osborne, R., Vos, T., Buchbinder, R., Woolf, A., & March, L. (2014). The global burden of hip and knee osteoarthritis: Estimates from the global burden of disease 2010 study. *Annals of the Rheumatic Diseases*, *73*(7), 1323–1330. https://doi.org/10.1136/annrheumdis-2013-204763

Herbold, J. A., Bonistall, K., Blackburn, M., Agolli, J., Gaston, S., Gross, C., Kuta, A., & Babyar, S. (2014). Randomized controlled trial of the effectiveness of continuous passive motion after total knee replacement. *Archives of Physical Medicine and Rehabilitation*, *95*(7), 1240–1245. https://doi.org/10.1016/j.apmr.2014.03.012

Hunter, D. J., Schofield, D., & Callander, E. (2014). The individual and socioeconomic impact of osteoarthritis. *Nature Reviews Rheumatology*, *10*(7), 437–441. https://doi.org/10.1038/nrrheum.2014.44

Johnston, R. C., Fitzgerald, R. H., Jr., Harris, W. H., Poss, R., Müller, M. E., & Sledge, C. B. (1990). Clinical and radiographic evaluation of total hip replacement: A standard system of terminology for reporting results. *The Journal of Bone & Joint Surgery*, *72*(2), 161–168.

Kim, M. S., Kim, J. J., Kang, K. H., Ihm, J. S., & In, Y. (2023). Ankle pain after medial opening-wedge high tibial osteotomy in patients with knee osteoarthritis and concurrent ankle osteoarthritis. *The American Journal of Sports Medicine*, *51*(2), 494–502. https://doi.org/10.1177/03635465221143999

Lee, B. C., Moon, C. W., Choi, W. S., Kim, Y. M., Joo, Y. B., Lee, D. G., Lee, S. J., Choi, E. S., Ji, J. H., Suh, D. W., & Cho, K. H. (2022). Clinical evaluation of usefulness and effectiveness of sitting type continuous passive motion machines in patients with total knee arthroplasty: A study protocol for a single-blinded randomized controlled trial. *BMC Musculoskeletal Disorders*, *23*(1), Article 565. https://doi.org/10.1186/s12891-022-05507-2

Mille, M. A., McClement, J., & Lauer, S. (2023). Physiotherapeutic strategies and their current evidence for canine osteoarthritis. *Veterinary Sciences*, *10*(1), Article 2. https://doi.org/10.3390/vetsci10010002

Neogi, T. (2013). The epidemiology and impact of pain in osteoarthritis. *Osteoarthritis and Cartilage*, *21*(9), 1145–1153. https://doi.org/10.1016/j.joca.2013.03.018

Parra, D., Contreras, J. D., & Garcia, J. I. (2022). Fault detection and insulation model-based of a teleoperated technical aid for knee rehabilitation using bond graph. *IFAC-PapersOnLine*, *55*(19), 25–30. https://doi.org/10.1016/j.ifacol.2022.09.179

Rahman, R. U., Rashid, A., Shahnaz, I., Murtaza, S. R., Ahmed, A., Ali, M. R., Ejaz, K.,Tabrez, R. A., Khan, A. Q., & Khan, S. J. (2018). Smart passive rehabilitative device to enhance knee range of motion. In *2018 IEEE-EMBS Conference on Biomedical Engineering and Sciences (IECBES)* (pp. 161–165). IEEE. https://doi.org/10.1109/IECBES.2018.8626649

Saputra, M. K., & Iskandar, A. A. (2011). Development of automatic continuous passive motion therapeutic system. In *2011 2nd International Conference on Instrumentation, Communications, Information Technology, and Biomedical Engineering* (pp. 376–379). IEEE. https://doi.org/10.1109/ICICI-BME.2011.6108630

Sun, J., Gao, S., Liu, W., Kong, F., & Li, X. (2023). Design and static analysis of new deployable mechanisms based on the four-bar slider–crank mechanism. *Mechanics Based Design of Structures and Machines*, *51*(11), 6204–6226. https://doi.org/ 10.1080/15397734.2022.2038617

Szabo, D. A., Cartala, V., & Neagu, N. (2023). New technologies used in the rehabilitation of knee pathologies. *Health, Sports & Rehabilitation Medicine*, *24*(3), 154–162. https://doi.org/10.26659/pm3.2023.24.3.154

Umchid, S., & Taraphongphan, P. (2016). Design and development of a smart continuous passive motion device for knee rehabilitation. In *2016 9th Biomedical Engineering International Conference (BMEiCON)* (pp. 1–5). IEEE. https://doi.org/10.1109/BMEiCON.2016.7859616

Wu, X., Sun, Y., Wang, Y., & Chen, Y. (2021). Correlation dimension and bifurcation analysis for the planar slider-crank mechanism with multiple clearance joints. *Multibody System Dynamics*, *52*(1), 95–116. https://doi.org/10.1007/s11044-020-09769-3